

TURBULENCE IN THE UPPER ATMOSPHERE

by C. G. Justus and H. D. Edwards

Georgia Tech Project A652-001

Contract No. NsG 304-63

FACILITY FORM 802	N65 19753	
	(ACCESSION NUMBER)	(THRU)
	56	1
	(PAGES)	(CODE)
	W57258	13
	(NASA CR OR TMX OR AD NUMBER)	(CATEGORY)

Prepared for  
National Aeronautics and Space Administration  
Washington 25, D. C.

GPO PRICE \$ \_\_\_\_\_

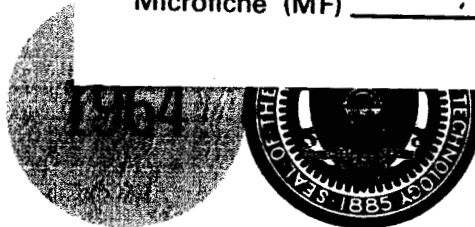
OTS PRICE(S) \$ \_\_\_\_\_

UNPUBLISHED PRELIMINARY DATA

Hard copy (HC) 3.00

Microfiche (MF) .50

July 1964



Engineering Experiment Station  
GEORGIA INSTITUTE OF TECHNOLOGY  
Atlanta, Georgia

REPORTS CONTROL No. 6

TURBULENCE IN THE UPPER ATMOSPHERE\*

By

C. G. Justus and H. D. Edwards

Georgia Tech Project A652-001

Prepared for

National Aeronautics and Space Administration  
Washington 25, D. C.

Contract No. NsG 304-63

July 1964

\*The studies reported here were also supported by the Air Force Cambridge Research Laboratories under Contract Af19(628)3305.

## SCIENTISTS

The following scientists contributed to the technical work

1. Dr. H. D. Edwards - - - - - Project Director
2. Dr. W. M. Schofield - - - - - Research Physicist
3. R. N. Fuller- - - - - Research Assistant
4. C. G. Justus- - - - - Graduate Research Assistant
5. A. J. Lineberger- - - - - Graduate Research Assistant
6. W. B. Moseley - - - - - Graduate Research Assistant
7. J. M. Reynolds- - - - - Graduate Research Assistant
8. J. R. Williams- - - - - Graduate Research Assistant
9. A. Woodrum- - - - - Graduate Research Assistant
10. H. W. Morgan- - - - - Student Assistant
11. J. E. Westmoreland- - - - - Student Assistant
12. B. H. Zellner - - - - - Student Assistant

## TABLE OF CONTENTS

	Page
SCIENTISTS. . . . .	2
ABSTRACT. . . . .	4
INTRODUCTION. . . . .	5
SCALES OF THE MOTION. . . . .	8
Vertical Autocorrelation Scale of the Mean Winds	
Motion Spectrum Scale of the Mean Winds	
Motion Spectrum of the Turbulent Winds	
The Mixing Length Scale	
Scale of the Smallest Eddies	
Correlation Scales of the Turbulent Velocities	
Dissipation Length Parameter from Turbulent Winds	
Globule Size Scales and the Globule Cut Off Altitude	
Time Scales of the Motion	
Summary	
ENERGY BALANCE OF THE MOTION. . . . .	36
CRITERIA FOR THE ONSET OF TURBULENCE. . . . .	44
Reynold' Criterion	
Richardson's Criterion	
Townsend's Criterion	
Layzer's Criterion	
Observations on Chemical Release Wind Data	
CONCLUSIONS . . . . .	49
REFERENCES. . . . .	54

## TURBULENCE IN THE UPPER ATMOSPHERE

C. G. Justus and H. D. Edwards  
Georgia Institute of Technology  
Atlanta, Georgia

### ABSTRACT

19753

By direct investigation of fluctuating turbulent velocities determined from chemical releases, data have been obtained which indicate that turbulence observed up to altitudes near 105 km is ambient turbulence, produced by wind shears. This turbulence is isotropic only for scales  $\approx 1$  km or less. The smallest eddies are on the order of 20 m in size with characteristic velocities and times of about 2 m/sec and 10 sec. The largest eddies observed are about 6 km in size with characteristic velocities and times of about 15 m/sec and 400 sec. It is thought that tidal waves and gravity wave components may account for the major portion of all velocity fluctuations with size scales greater than 6 km.

The turbopause, or upper height limit of turbulence of the scales observed, usually occurs within  $\pm 5$  km of the 105 km level. This cutoff altitude appears to be the result of the rate of energy supplied by the wind shears becoming too small to maintain the turbulence in the presence of a dissipation rate which is increasing rapidly with altitude.

Growth measurements on diffusing globules produced in the chemical release clouds indicates that the Batchelor form of turbulent diffusion is applicable in this height range.

AUTHOR →

## INTRODUCTION

Edwards et al (1963) and other groups have reported that chemical release clouds usually become globular in appearance below some altitude, usually around 105-110. It is presumed that these globules are associated with turbulence but there remains some question (Nawrocki and Papa (1963) and Cote (1962) ) as to whether this turbulence is naturally occurring ambient turbulence or is in some way produced by either the ejection mechanism or a reaction of the ejection vehicle with the ambient.

In the following report an attempt is made to examine the turbulence quantitatively, comparing results whenever possible with the predictions of existing turbulence theories. It is hoped that these results will shed some light on this problem of the exact cause of the turbulence.

In an attempt to unify the thinking with regard to turbulence and turbulent eddies Stewart (1959) proposed the following definitions:

Turbulence - "A fluid is said to be turbulent if each component of the velocity is distributed irregularly and aperiodically in time and space, if the flow is characterized by a transfer of energy from larger to smaller scales of motion, and if the mean separation of neighboring fluid particles tends to increase with time."

Eddy - An eddy is "a volume of fluid moving more or less coherently with respect to the mean flow."

These definitions exclude from the realm of turbulence such two dimensional phenomena as vortex sheets, whirlpools, convection cells, and internal waves.

Turbulent motion is in many ways analogous to the random molecular motions responsible for the phenomena of viscosity, diffusion, and conductivity in

gases. There are, however, several differences between these two types of motion. First, a molecule is under the influence of a very small number of other molecules in the gas and each molecule moves about somewhat freely, whereas a fluid element in turbulent motion cannot move independently of the general motion of the other fluid elements. Turbulent motion is less random, or more ordered, than molecular motions. Secondly, turbulent motion requires a continuous source of energy to maintain it. If the air is thermally unstable, that is, cool air over warm air, the potential energy of the unstable arrangement can supply the turbulence. In a stably stratified region of the atmosphere, such as that above 85 km, wind shears provide the only source of energy for maintaining turbulence.

According to standard turbulence theories (See Townsend (1956).) the eddies in a turbulent field have a spectrum of sizes ranging from the largest eddies, which are being supplied with energy from the source, through the intermediate sized energy containing eddies on down to the smallest eddies, which lose their energy by the effects of viscosity. Each eddy size interacts extensively only with other eddies of neighboring size so that eddies containing energy lose energy to only slightly smaller eddies which in turn lose their energy to still slightly smaller eddies, and so on until the smallest eddy size is reached.\* The effect of viscosity is to remove energy from only one size of eddies and not to redistribute it among other eddy sizes, although the viscous stresses can convert energy into heat or accelerate neighboring particles.

\*

"Big whirls have little whirls that feed on their velocity  
And little whirls have lesser whirls, and so on to viscosity."

- L. F. Richardson

Previous investigators have employed two primary means of investigating the ionospheric altitude region near 100 km with regard to the existence of turbulence. These methods are (1) direct investigation of the turbulent velocity fluctuations and (2) investigation of the diffusion characteristics of materials released into the atmosphere.

Up until the present time the first method has been used only in connection with radio echo observations of meteor trails such as those by Greenhow and Neufeld (1959a, 1959b, 1960). Here the instantaneous horizontal wind is  $U + u$  where  $U$  is the mean horizontal wind determined, for example, by averaging all the wind determinations over a one hour period, and  $u$  is considered to be the instantaneous turbulent wind fluctuation.

Accurate methods have now been developed for determining winds by triangulation and tracking of artificial chemical clouds released into the atmosphere by rockets. (See Albritton, et al (1962); Justus, et al (1964a, 1964b).) Using these methods it is possible to measure instantaneous wind velocities over a range of altitudes. Averaging of the wind data allows the determination of the north-south and east-west components of the mean winds,  $U(z)$  and  $V(z)$ , as functions of altitude,  $z$ . The vertical component of mean wind  $W(z)$  is considered to be zero. The instantaneous velocity components determined at a height  $z$  are then  $U(z) + u(z)$ ,  $V(z) + v(z)$ , and  $w(z)$ , where  $u$ ,  $v$ , and  $w$  are considered to be the instantaneous components of the turbulent velocity fluctuations. Note that  $w$  is not necessarily zero. The equivalent notation  $(u_1, u_2, u_3)$  is sometimes used instead of  $(u, v, w)$  for the components of the turbulent velocity.



## SCALES OF THE MOTION

### Vertical Autocorrelation Scale of the Mean Winds

Since the mean winds  $U(z)$  and  $V(z)$  are not static or uniform there can also be scales associated with the mean wind field. Liller and Whipple (1954) performed a vertical autocorrelation analysis on the mean wind profile determined from visual meteor trails. The vertical autocorrelation coefficient  $G_U(\delta z)$  is given by

$$G_U(\delta z) = \frac{\sum [U(z) U(z + \delta z)]}{\{\sum [U(\delta)]^2 \sum [U(z + \delta z)]^2\}^{\frac{1}{2}}} \quad (1)$$

for the  $U$  component of the mean wind profile. A correlation coefficient for the  $V$  component is given by substitution of  $V$  for  $U$  in (1). The sums in (1) run over all pairs of data points separated by a vertical distance  $\delta z$ , or the sums may be replaced by integration if  $U$  is considered as a continuous function. Physically, this analysis determines the degree of correlation between the wind profile and the wind profile displaced by an amount  $\delta z$  in the vertical direction. The values of the coefficient  $G$  should start at  $+1$  for  $\delta z = 0$ , go to  $0$  for  $\delta z = \frac{1}{4}\lambda$ , and on to  $-1$  for  $\delta z = \frac{1}{2}\lambda$ , where  $\lambda$  is the vertical "wave length" of the mean wind component profile.

Liller and Whipple obtained an average value of 5.2 km for  $L_V$ , the distance  $\delta z$  for which  $G = 0$ . This value is applicable for the height region somewhere between 82 and 113 km. Using the Liller and Whipple wind data Hines (1960) subtracted a constant shear wind from the wind profile and multiplied the residual wind by a height varying scaling factor to compensate for the increase in amplitude of the wind with altitude. After this alteration Hines obtained a value of 4.0 km for  $L_{V2}$ , the modified zero autocorrelation distance.

Wind data obtained from about 30 chemical releases launched from Eglin AFB, Florida during 1962 and 1963 has been put to vertical autocorrelation analysis. The data was broken up into three height intervals 70-90 km, 90-115 km, and 115-170 km. The representative mean altitude for each height range was 81 km, 104 km and 130 km. Three types of zero autocorrelation lengths were calculated:  $L_v$  for unmodified data,  $L_{v1}$  for residual winds after subtraction of a representative constant shear wind, and  $L_{v2}$  for the residual winds multiplied by a height scaling factor.

Figure 1 shows a typical set of results for  $G_U$  and  $G_V$ . They were obtained from a release occurring at 05:15 CST on 16 October 1962 and covering an altitude range of 92-106 km. The autocorrelation curve  $G_V(\delta z)$  crosses zero at  $L_v = 8.6$  km, the corresponding value for  $G_U(\delta z)$  is 7.5 km.

Figure 2 shows the average results for  $L_v$ ,  $L_{v1}$ , and  $L_{v2}$  in each of the three height ranges. The Liller and Whipple value agrees well with the  $L_v$  data and the Hines value shows good agreement with the  $L_{v2}$  data. All three L scales show an increase in magnitude with increasing altitude, the rate of increase being about the same in all three cases.

Zimmerman (1964) has suggested that the vertical scale of the mean winds is connected with the scale height, H. A graph of H versus altitude is also included in Figure 2 for comparison. It appears that there is reasonable correspondence between the values for  $L_v$  and H in the height range from 90-105 km but the  $L_v$  values fall below the values for H in the height regions above and below this.

#### Motion Spectrum Scale of the Mean Winds

Another method for obtaining information about the scale of the mean

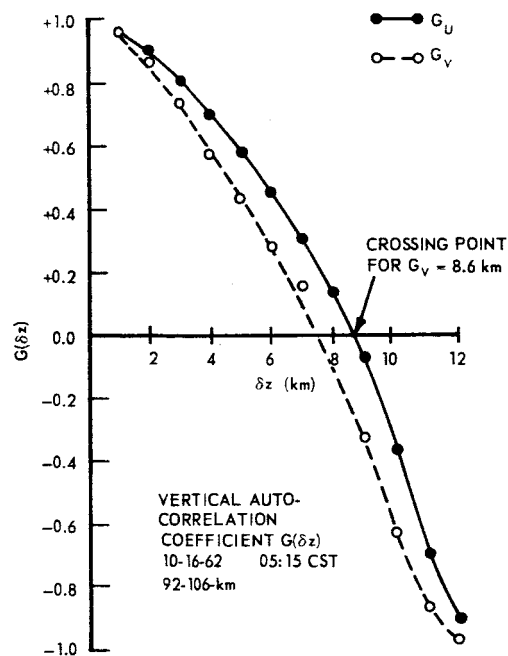


Figure 1. Typical Vertical Autocorrelation Curve.

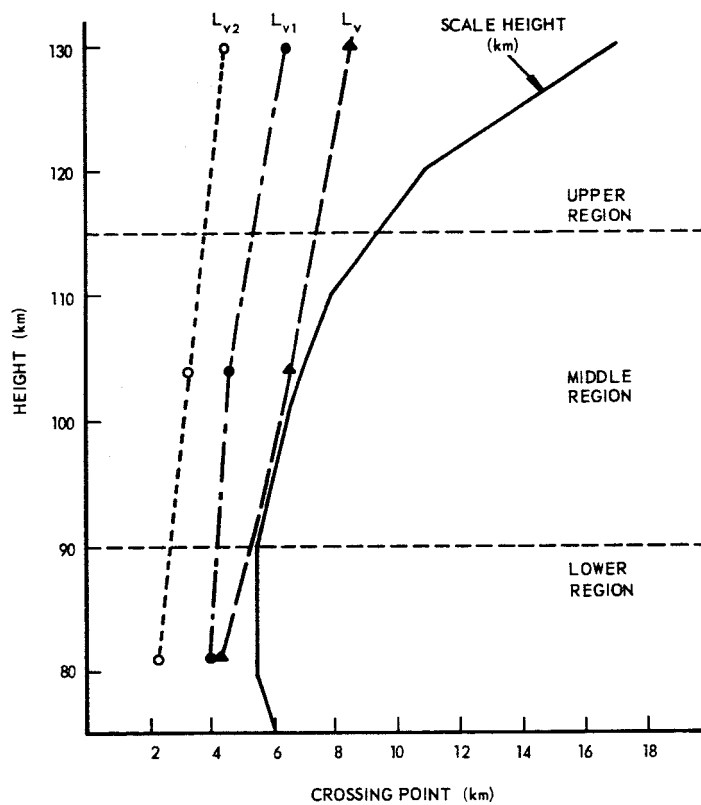


Figure 2. Vertical Autocorrelation Scales Versus Altitude.

winds is the evaluation of the point  $\delta z = L_s$  at which the motion spectrum function is a maximum. The motion spectrum function,  $F(\delta z)$ , is obtained by averaging the square velocity differences, that is

$$F(\delta z) = \langle [U(z) - U(z + \delta z)]^2 \rangle \quad (2)$$

and similarly for the V component, where the average is taken over all data points separated by a height difference  $\delta z$ .

Blamont and de Jager (1961, 1962) report results of a motion spectrum analysis of four sodium trails showing that for small values of  $\delta z$ ,  $F(\delta z) \sim (\delta z)^n$  where  $n = 1.4 \pm 0.2$ . They also report that  $F(\delta z)$  graphs show maxima which correspond with the vertical correlation length. Evaluation of the point  $\delta z = L_s$  at which these maxima occur thus provides another method of estimating the vertical scale of the mean winds.

The chemical release wind data used in the vertical autocorrelation analysis was also analyzed in a similar fashion for motion spectrum features, the data being divided into three height ranges, roughly, 70 to 93 km, 93 to 112 km and 112 to 143 km. Figure 3 shows the results of a typical motion spectrum analysis. These data are from a release occurring 3 December 1962 at 18:50 CST and are valid for the height region 112-143 km. It is seen that for small  $\delta z$  the exponent  $n$  for the spectrum function power law is 1.71. A maximum in  $F(\delta z)$  occurs at  $\delta z = 12$  km, thus  $L_s$  is 12 km for this graph.

Figure 4 shows the averaged results of the evaluation of the maximum point  $L_s$  for each of the three altitude regions. The  $L_s$  values, like the  $L_v$  vertical autocorrelation scales, agree with the scale height, especially in the lower and middle height regions,  $L_v$  being somewhat less than the scale height in the upper region.

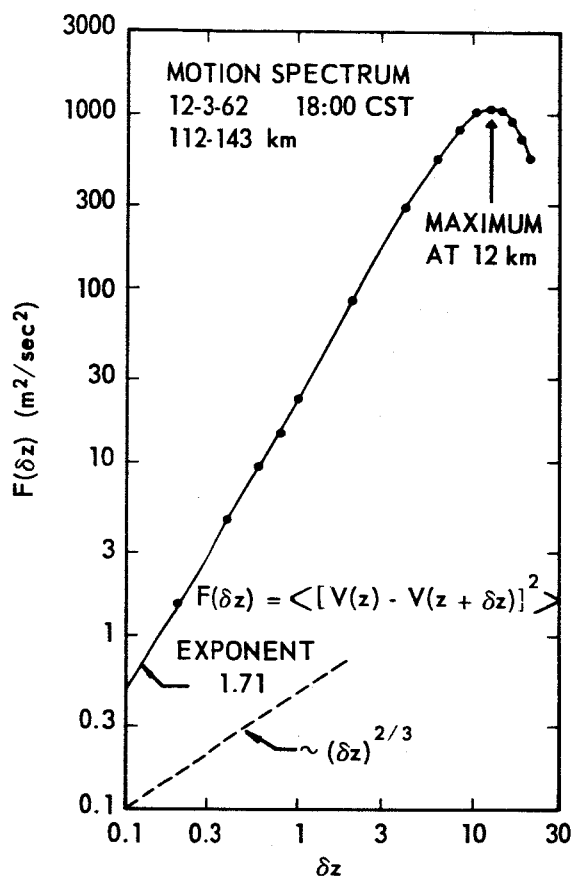


Figure 3. Typical Motion Spectrum Curve.

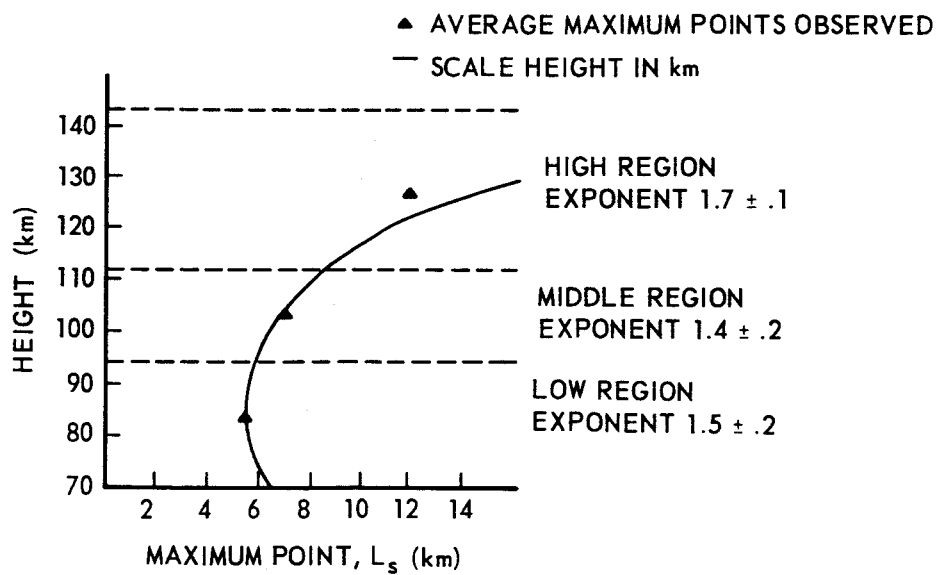


Figure 4. Motion Spectrum Scale Versus Altitude.

Figure 4 also tabulates the average exponents observed for  $F(\delta z)$ . The exponent is almost constant over the altitude range examined, increasing only slightly with increasing altitude.

Zimmerman (1962) has pointed out that the motion spectrum analysis by Blamont and de Jager (1961), yielding an exponent of  $1.4 \pm .2$  is in agreement with the shear turbulence theory of Tchen (1954) which predicts an exponent of  $4/3$ . Zimmerman also shows that the data of Blamont and de Jager support Tchen's theory with regard to the energy spectrum. He calculates the average turbulent energy per unit mass  $E$ , given by

$$E = | \langle U^2(z) \rangle - \langle U^2(z + \delta z) \rangle | \quad (3)$$

and shows that  $E \sim \delta z^{2/3}$  for small  $\delta z$ .

Roper and Elford (1963) report that the motion spectrum function  $F(\delta z)$  is proportional to  $\delta z^{4/3}$  if only height separation is considered, but that  $F(\delta r)$  is proportional to  $\delta r^{2/3}$  if  $F$  is considered as a function of the total separation  $\delta r$ .

Analysis of chemical release wind data is presently underway to calculate  $F(\delta r)$  and  $E$ . Preliminary results tend to confirm the conclusions of Zimmerman, and Roper and Elford.

#### Motion Spectrum of the Turbulent Winds

Based on work by Kolmogoroff (1941) it was shown by Batchelor (1947) that the turbulent motion spectrum function

$$f(\underline{\delta r}) = \langle [u(\underline{r}) - u(\underline{r} + \underline{\delta r})]^2 \rangle \quad (4a)$$

obeys the relationship

$$f(\delta r) = C_1 (\epsilon_t \delta r)^{2/3} \left( 1 + \frac{\delta r_1}{3 \delta r^2} \right) \quad (4b)$$

where  $C_1$  is an absolute constant,  $\delta r$  is the magnitude of  $\delta \underline{r}$  and  $\delta r_1$  is the component of  $\delta \underline{r}$  in the direction of the turbulent wind component  $u$ . See Sutton (1953) for a summary of the work of Kolmogoroff and Batchelor on this topic.

For most purposes (4b) may be written as

$$f(\delta r) \sim (\delta r)^{2/3} \quad (5)$$

which is known as Kolmogoroff's Law.

Turbulent winds determined from 13 chemical releases launched from Eglin AFB, Florida from 1959 to 1963 have been analyzed to determine the applicability of (5) to the turbulence of the upper atmosphere. The results, shown in Figure 5, indicate that Kolmogoroff's Law is not followed for  $\delta r \gtrsim 1$  km.

The figure indicates that the law may be followed for  $\delta r < 1$  km but the data points are too uncertain to be conclusive. Kolmogoroff's Law is based on the assumption of isotropic turbulence and it is shown later that the turbulence may be isotropic only for eddy scales of 1 km or less.

#### The Mixing Length Scale

An analogy has been made between molecular and turbulent motions by introducing the concept of mixing length. According to the mixing length idea of turbulent motion, eddies transport momentum from one level of the flow to another and the transport of momentum from the level  $z$  to the level

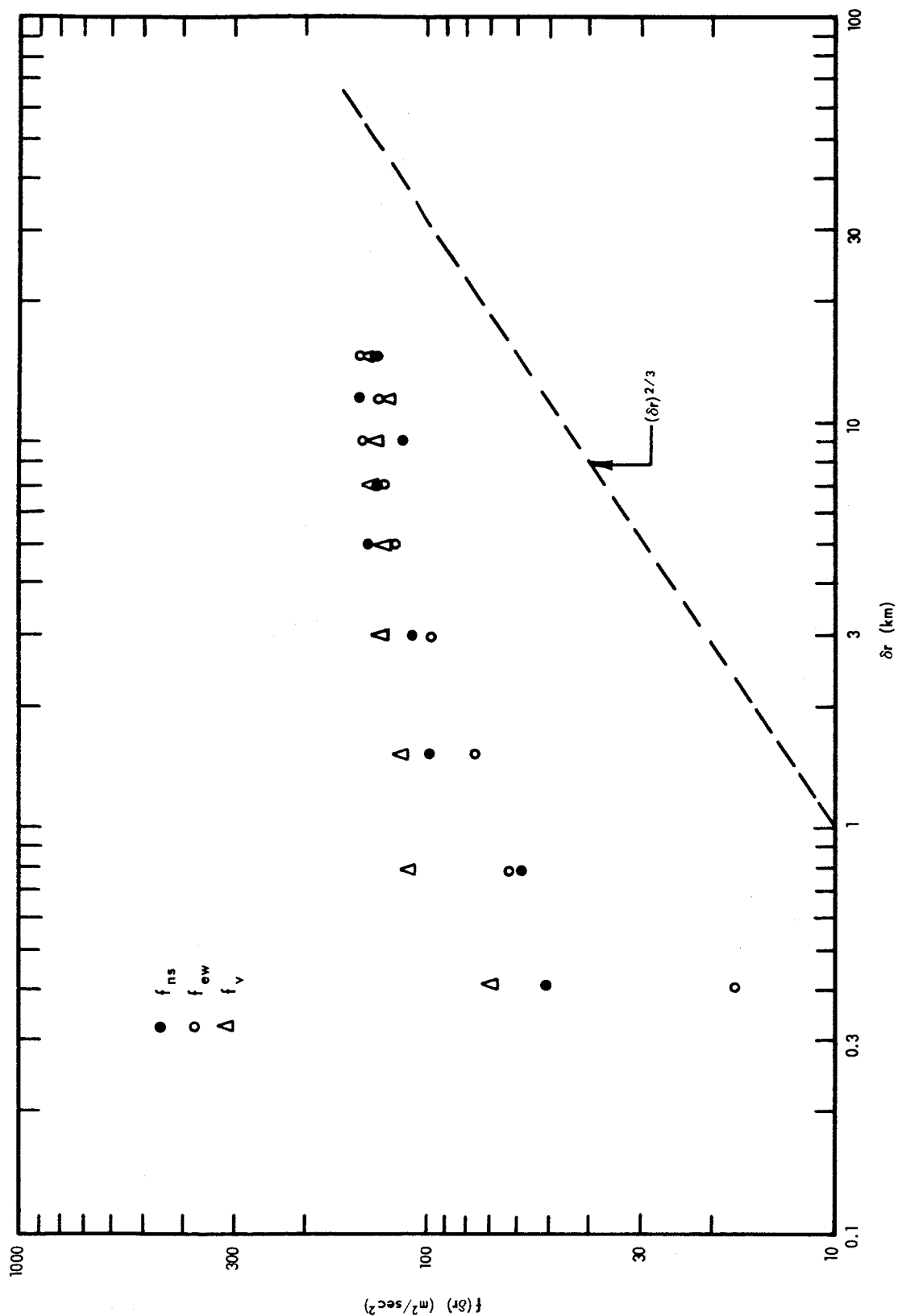


Figure 5. Motion Spectrum of Turbulent Winds.



$z + L_m$  produces a fluctuation,  $u$ , in the mean velocity,  $U$ , given by

$$u = U(z + L_m) - U(z) \approx L_m \frac{\partial U}{\partial z} \quad (6)$$

here  $L_m$  is the mixing length. Thus the magnitude of the mixing length can be found approximately by

$$L_m \approx \frac{u}{\left(\frac{\partial U}{\partial z}\right)} \quad (7)$$

Figure 6 shows the averaged results obtained from several chemical releases. The mixing length scale is seen to remain fairly constant from 92 to 108 km at a value close to 0.8 km and then increase rapidly above 108 km to about 3.3 km at 112 km altitude.

#### Scale of the Smallest Eddies

Standard theories of homogeneous turbulence provide a method of evaluating the scale of the smallest, energy dissipating eddies. The size of these eddies,  $l_e$ , should be given by

$$l_e = \left(\frac{\eta^3}{\epsilon}\right)^{\frac{1}{4}} \quad (8)$$

where  $\eta$  is the kinematic viscosity of the atmosphere, and  $\epsilon$  is either the rate,  $\epsilon_s$ , at which the wind shears supply energy to the turbulence or the rate,  $\epsilon_t$ , at which the turbulence is dissipating energy as heat. For isotropic turbulence  $\epsilon_s$  is presumed to be approximately equal to  $\epsilon_t$ . The kinematic viscosity can be evaluated up to a height of 90 km from values given in the U. S. Standard Atmosphere (1962) and above this altitude from the formula used for generating the Standard Atmosphere tables

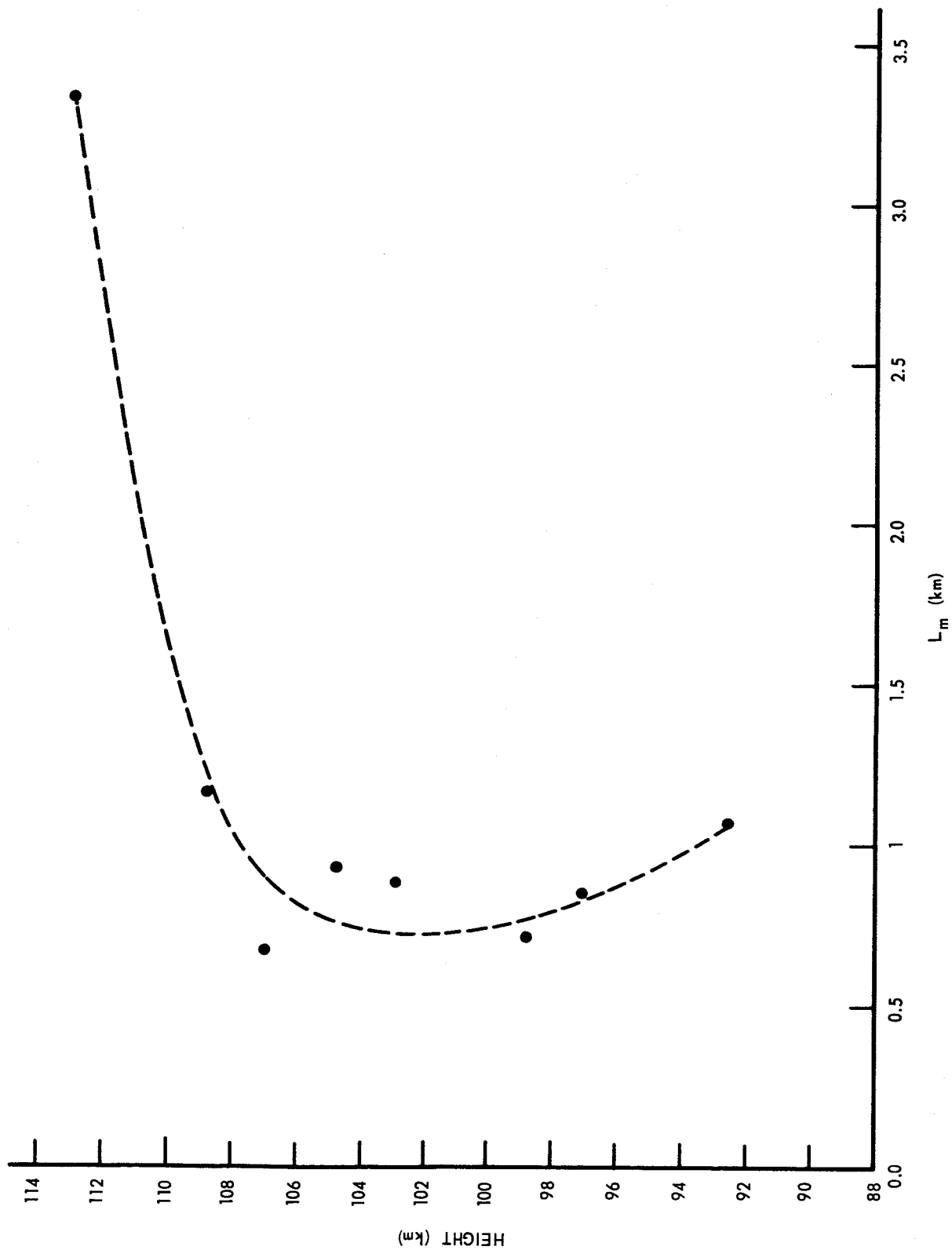


Figure 6. Mixing Length Versus Altitude.

$$\eta = \frac{\beta T^{3/2}}{\rho (T + S)} \quad (\text{m}^2/\text{sec}) \quad (9)$$

where  $\beta = 1.458 \times 10^{-6}$ ,  $S = 110.4$  °K, and  $T$  and  $\rho$  are the atmospheric temperature and density in °K and  $\text{kg}/\text{m}^3$ .

Actual evaluations of  $\epsilon_t$  and  $\epsilon_s$  show that these quantities are not the same throughout the upper atmosphere. (See later sections of this report for evaluation of these parameters.) Tables 1 and 2 show values of  $l_e$  calculated from  $\epsilon_s$  and  $\epsilon_t$  for three altitudes. Both sets of values show that  $l_e$  is of the order of 10 m and that  $l_e$  is increasing in magnitude with increasing altitude.

TABLE I  
VALUES OF  $l_e$  USING  $\epsilon_s$

Height (km)	$\eta$ ( $\text{m}^2/\text{sec}$ )	$\epsilon_s$ ( $\text{m}^2/\text{sec}^3$ )	$l_e$ (m)
92	5.7	0.30	5
100	28	0.37	16
108	120	0.46	44

TABLE 2  
VALUES OF  $l_e$  USING  $\epsilon_t$

Height (km)	$\eta$ ( $\text{m}^2/\text{sec}$ )	$\epsilon_t$ ( $\text{m}^2/\text{sec}^3$ )	$l_e$ (m)
92	5.7	0.012	11
100	28	0.14	20
108	120	1.1	35

### Correlation Scales of the Turbulent Velocities

The general double-velocity correlation coefficient  $g_{ij}(\underline{x}; \underline{r})$  is given by

$$g_{ij}(\underline{x}; \underline{r}) = \frac{\langle u_i(\underline{x}) u_j(\underline{x} + \underline{r}) \rangle}{[\langle u_i^2(\underline{x}) \rangle \times \langle u_j^2(\underline{x} + \underline{r}) \rangle]^{\frac{1}{2}}} \quad i, j = 1, 2, 3 \quad (10)$$

where now  $\underline{x}$  is the position vector  $(x_1, x_2, x_3)$ ,  $\underline{r}$  is the vector  $(r_1, r_2, r_3)$  and  $u_1, u_2, u_3$  are the components of the turbulent velocity previously denoted by  $u, v$ , and  $w$ , and the mean values are taken with respect to time. As seen from the defining formula, the correlation coefficient  $g_{ij}(\underline{x}; \underline{r})$  serves as a measure of the degree of correlation between the turbulent velocity fluctuations  $u_i(\underline{x})$  and  $u_j(\underline{x} + \underline{r})$ , and therefore  $g_{ij}(\underline{x}; \underline{r}) = 1$  for  $\underline{r} = 0$  and  $g_{ij}(\underline{x}; \underline{r})$  approaches 0 as  $|\underline{r}|$  approaches the size of the largest eddies.

Of special interest are the particular set of one-dimensional correlation coefficients  $g_{ii}(\underline{x}; r, 0, 0)$ ,  $g_{ii}(\underline{x}; 0, r, 0)$  and  $g_{ii}(\underline{x}; 0, 0, r)$  or, if the correlation coefficients are presumed to be independent of the position in the turbulent field, the coefficients may be denoted by  $g_{ii}(r, 0, 0)$ ,  $g_{ii}(0, r, 0)$  and  $g_{ii}(0, 0, r)$ . If the correlation coefficient is also isotropic the coefficient may be characterized by the single function  $g(r)$  given by

$$g(r) = g_{11}(r, 0, 0) = g_{22}(0, r, 0) = g_{33}(0, 0, r)$$

An integral scale of the turbulent motion,  $L_i$  is defined to be

$$L_i = \int_0^\infty g(r) dr \quad (11)$$

The scale of the largest eddies may be defined as the point  $r = L_0$  at which  $g(r)$  is first zero, or, more loosely, the point  $L_0$  at which an extrapolation of  $g(r)$  is zero should  $g(r)$  remain positive.

It can be shown (Taylor (1938) ) that to second order in  $r$ ,  $g(r)$  is given by

$$g(r) = \frac{\langle (\frac{\partial u}{\partial r})^2 \rangle}{2 \langle u^2 \rangle} r^2 = 1 - \frac{r^2}{L_p^2} \quad (12)$$

where  $u$  is the turbulent velocity component in the appropriate direction to correspond to  $r$ , and

$$L_p = \left[ \frac{2 \langle u^2 \rangle}{\langle (\frac{\partial u}{\partial r})^2 \rangle} \right]^{\frac{1}{2}} \quad (13)$$

is the dissipation length parameter.  $L_p$  is considerably larger in magnitude than the scale of the smallest, energy dissipating eddies.  $L_p$  is a length corresponding to eddies which contain a negligible portion of the total energy and are responsible for a negligible part of the total dissipation of energy as heat.

Townsend (1956) gives a relation showing that the scale of the dissipating eddies, here denoted by  $l_c$ , is given by

$$l_c^2 = \frac{L_p^3}{10 \sqrt{15} L_0} \quad (14)$$

As an approximation to  $g_{ii}(r, 0, 0)$ ,  $g_{ii}(0, r, 0)$  and  $g_{ii}(0, 0, r)$  for  $i = 1, 2$  (the horizontal components), Greenhow and Neufeld (1959b) calculated

$$g(r, z) = \frac{\sum [u'(\underline{x}) u'(\underline{x} + \underline{r})]}{[\sum u'^2(\underline{x}) \sum u'^2(\underline{x} + \underline{r})]^{\frac{1}{2}}} \quad (15)$$

where, here,  $u'$  is the horizontal component of the turbulent velocity as defined in the introduction for the meteor type data,  $\underline{r}$  is the vector with magnitude  $r$  and vertical component  $z$ , and the summations extend over all positions  $\underline{x}$  at which wind determinations were made.

Greenhow and Neufeld plot their determination of  $g(r, z)$  versus both  $r$  and  $z$  and conclude from these graphs that the vertical scale of the largest eddies is 6 km. They report that consideration of echo pairs of the same height separation but different horizontal separations leads to a horizontal rate of decay in the correlation which indicates a horizontal scale of the order of 100 to 200 km. Using 150 km for their value of  $L_0$  and 2.4 km as their value of  $L_p$ , they deduce from (14) a size  $l_c \approx 50$  m for the smaller eddies.

Wind data from 13 chemical releases launched from Eglin AFB, Florida between 1959 and 1963 have been used to calculate correlation coefficients analogous to the Greenhow and Neufeld approximation by computing  $g(r, z)$  by (15), where now  $u'$  stands for the horizontal component of the turbulent velocity  $(u^2 + v^2)^{\frac{1}{2}}$  with a + or - sign attached according to whether the magnitude of the instantaneous wind is greater or less than the magnitude of the mean wind.

A horizontal correlation coefficient  $g(r, h)$  can be defined by

$$g(r, h) = \frac{\sum [u'(\underline{x}) u'(\underline{x} + \underline{r}')] }{[\sum u'^2(\underline{x}) \sum u'^2(\underline{x} + \underline{r}')] } \quad (16)$$

where  $\underline{r}'$  is a vector with magnitude  $r$  and horizontal component  $h$ , and the summation extends over all positions  $\underline{x}$  for which wind data were obtained such that  $z$ , the vertical component of  $\underline{r}'$ , is less than 1 km. Thus  $g(r, h)$  is an

approximation to  $g_{ii}(r, 0, 0)$  or  $g_{ii}(0, r, 0)$  and should yield information concerning the horizontal scale of the eddies.

Figure 7 and 8 show the averaged results of  $g(r, z)$  versus  $z$  and  $g(r, h)$  versus  $h$ . Both coefficients tend to zero at about 6 km, confirming the 6 km vertical scale deduced by Greenhow and Neufeld but indicating an equal 6 km horizontal scale instead of their 100-200 km value.

The horizontal scale of the mean winds, that is the horizontal distance over which the mean wind profile maintains some degree of correlation, is certainly greater than 100 km. Simultaneous wind data obtained from separate chemical release clouds some 100 km apart indicate that this scale may be of the order of 1000 km, since the wind profiles still have a positive correlation of about 0.9 for this 100 km separation. It could be that the horizontal scale that Greenhow and Neufeld reported was more nearly the scale of the mean winds than the scale of the turbulent winds. This discrepancy might result from their method of defining the turbulent components, which differs from the definition used with regard to the chemical release wind determinations.

Correlation coefficients similar to those in Figure 7 and 8 but calculated by using  $w$ , the vertical component of the turbulent velocity, in (15) and (16) instead of the horizontal component do not show a similar fall off in the correlation. Further investigation of this is planned and it is also planned that as a next approximation to the actual one-dimensional correlation coefficients the quantities  $g(r, h)$  and  $g(r, z)$  can be evaluated using complete set of components  $u$ ,  $v$ , and  $w$  in (15) and (16) instead of only horizontal and vertical components  $u'$  and  $w$ .

If the data from Figure 7 is used to estimate the integral scale of turbulence  $L_i$  one obtains a value  $L_i \approx 1$  km. The dissipation length para-

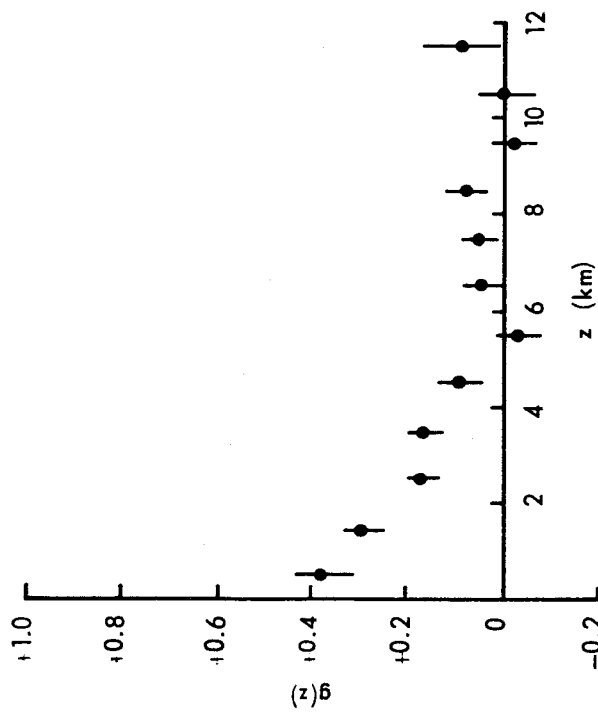


Figure 7. Spatial Correlation Coefficient for Vertical Separation.

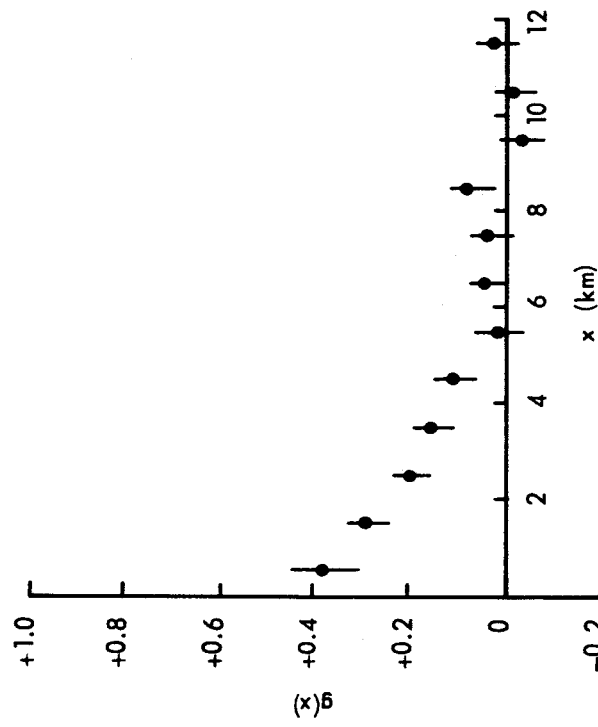


Figure 8. Spatial Correlation Coefficient for Horizontal Separation.



meter  $L_p$  is the point where a parabola  $g(h) = 1 - z^2/L_p^2$  passes through zero. If the data point  $z = 0.5$  km,  $g = 0.27$  is used from Figure 7 then

$$L_p = \left( \frac{z^2}{1 - g(z)} \right)^{\frac{1}{2}} = 0.6 \text{ km} \quad (17)$$

This value disagrees somewhat with the Greenhow and Neufeld value of 2.4 km because the data points of their correlation curve approach the value  $g = 1$  more closely for small  $z$ . The fact that the data points seen in Figures 7 and 8 do not seem to approach  $g = 1$  for  $z$  and  $h$  approaching zero may be due to the fact that an estimated r.m.s. error of about 3 - 5 m/sec is present in all of the wind determinations from the chemical releases whereas the r.m.s. value of the magnitude of the turbulent winds is about 16 m/sec. Since the errors constitute such a substantial percentage of the fluctuations being observed there may be some degree of destruction of correlation because of the errors. However it is interesting to note that Figures 7 and 8 show the same quantitative shape as correlation coefficients calculated by Townsend (1956) for a field of turbulence in which there are only two distinct eddy sizes.

If the values  $L_p = 0.6$  km and  $L_o = 6$  km are used in (14) the resultant value for  $l_c$  is 18 m. This value fits into the range of values shown in Tables 1 and 2 for the size of the smallest eddies. From the fact that a scale  $L_o$  of about 6 km results from both Figure 7 and Figure 8 data it would seem that the turbulence is almost isotropic, however, Dougherty (1961) has shown that the turbulence should be isotropic only in the range from  $l_c$  to  $l_i$ . The magnitude of  $l_c$ , the scale of the smallest eddies has been seen to be about 20 m, and  $l_i$  is given by

$$l_i = \frac{\varepsilon_t^{\frac{1}{2}}}{\omega_g^{3/2}} \quad (18)$$

where  $\epsilon_t$ , again is the rate of turbulent energy dissipation and  $\omega_g$  is the Brunt Vaisala frequency given by

$$\omega_g^2 = \frac{g}{T} \left( \frac{\partial T}{\partial z} + \frac{g}{C_p} \right) \quad (19)$$

where  $T$  is temperature,  $g$  is the acceleration of gravity,  $z$  is the vertical coordinate and  $C_p$  is the specific heat at constant pressure. The result (18) is based on Bolgiano's theory (1959, 1960) which hypothesizes that the isotropic inertial subrange exists only for scales between  $l_c$  and  $l_i$ , and that an anisotropic buoyancy subrange exists for scales between  $l_i$  and  $l_b$ . Data from which  $N$  can be computed are available in the U. S. Standard Atmosphere (1962). Using these values  $\omega_g$  is about  $2.4 \times 10^{-2} \text{ sec}^{-1}$  for  $90 \text{ km} < z < 115 \text{ km}$ . Using this value, Table 3 lists values for  $l_i$  for several altitudes, as determined by values of  $\epsilon_t$  from data presented later in this paper.

TABLE 3

Height (km)	$\epsilon_t$ ( $\text{m}^2/\text{sec}^3$ )	$l_i$ (km)
90	.0065	0.022
100	0.13	0.097
110	2.8	0.45
115	13	0.97

Thus, if the values of Table 3 are correct, the turbulence can be isotropic only for the smaller size eddies and indeed there is essentially no isotropic subrange below about 90 km. However, many globules in the height region 92-108

km remain approximately spherical up to sizes of 1 km or greater, but some of the globules larger than 1 km do become stretched into elliptical shapes. Therefore a more realistic value for the scale of isotropy may be about 1 km throughout the entire height region 90-110 km.

#### Dissipation Length Parameter from Turbulent Winds

Actual data on the turbulent wind components  $u$ ,  $v$  and  $w$  allow the calculation of the dissipation length parameter, now called  $L_t$ , by the relation (13)

$$L_t = \left[ \frac{2 \langle u^2 \rangle}{\langle \left( \frac{\partial u}{\partial x} \right)^2 \rangle} \right]^{\frac{1}{2}} \quad (20)$$

and similar relations obtained by replacing  $u$  by  $v$  or  $w$  and  $x$  by  $y$  or  $z$ . Here the partial derivatives have to be estimated by ratios of finite differences  $\Delta u$  and  $\Delta x$ .

Wind data obtained from 13 chemical releases shows an average value for  $L_t$  of 0.65 km, in very good agreement with the value of  $L_p$ , the dissipation length parameter determined from the correlation coefficient data.

#### Globule Size Scales and the Globule Cut-off Altitude

From observations on sodium trail releases near 100 km Blamont and de Jager (1961, 1962) report globules ranging in size from 70 meters to 1 km, with an average size of 0.5 km. Globule size data has been obtained from 13 chemical releases (primarily Cesium Nitrate-Aluminum) launched from Eglin AFB Florida between 1959 and 1963. Globules smaller than about 200 meters could not be measured from the photographs that were taken, but data on the growth

of 209 separate globules with diameters greater than 200 meters was obtained. Five of the releases had sufficient numbers of globules so that a size spectrum could be determined, that is, the number of globules of a given size could be plotted against globule diameters.

All five of these size spectrum plots have a peak at 0.7 km, and one has an additional peak at 1.2 km. The peak at 1.2 km occurs because of larger globules appearing in the height region 104-108 km. A large number of the individual growth curves of the globules level off at a diameter of about 0.7 km (or at 1.2 km for the higher ones) and then continue to increase (note Figure 9). Thus the reason for the peaks in the spectrum plots is that the growing globules tend to spend more time at this leveling off diameter than at other sizes. This leveling off scale for the globules,  $L_d$ , illustrated in Figure 10, increases from 0.4 km at  $97\frac{1}{2}$  km altitude to 0.75 km at 99 km and remains constant until at 106 km it begins to increase again and reaches 1.6 km at a height of 112 km. The mechanism that produces this leveling off in the growth curve is not known at the present.

The globular appearance of the chemical releases ceases at some altitude,  $H_t$ , called the turbopause altitude, between 100 and 115 km. Both point releases (i.e. chemicals released explosively at one or more points) and trail releases which covered an altitude range including  $H_t$  exhibited globules on that part of the cloud below  $H_t$  and were smooth above  $H_t$ . Blamont (1960) reported  $H_t$  to be at 102 km, and Manring (1962) at  $102 \pm 4$  km. A total of 56 observations on 19 chemical releases showed  $H_t$  to lie between the limits 96 and 115 km with an average of  $106 \pm 4$  rms.

Two of the releases produced one trail as the rocket ascended and another trail as the rocket descended. The up trails of these two releases showed

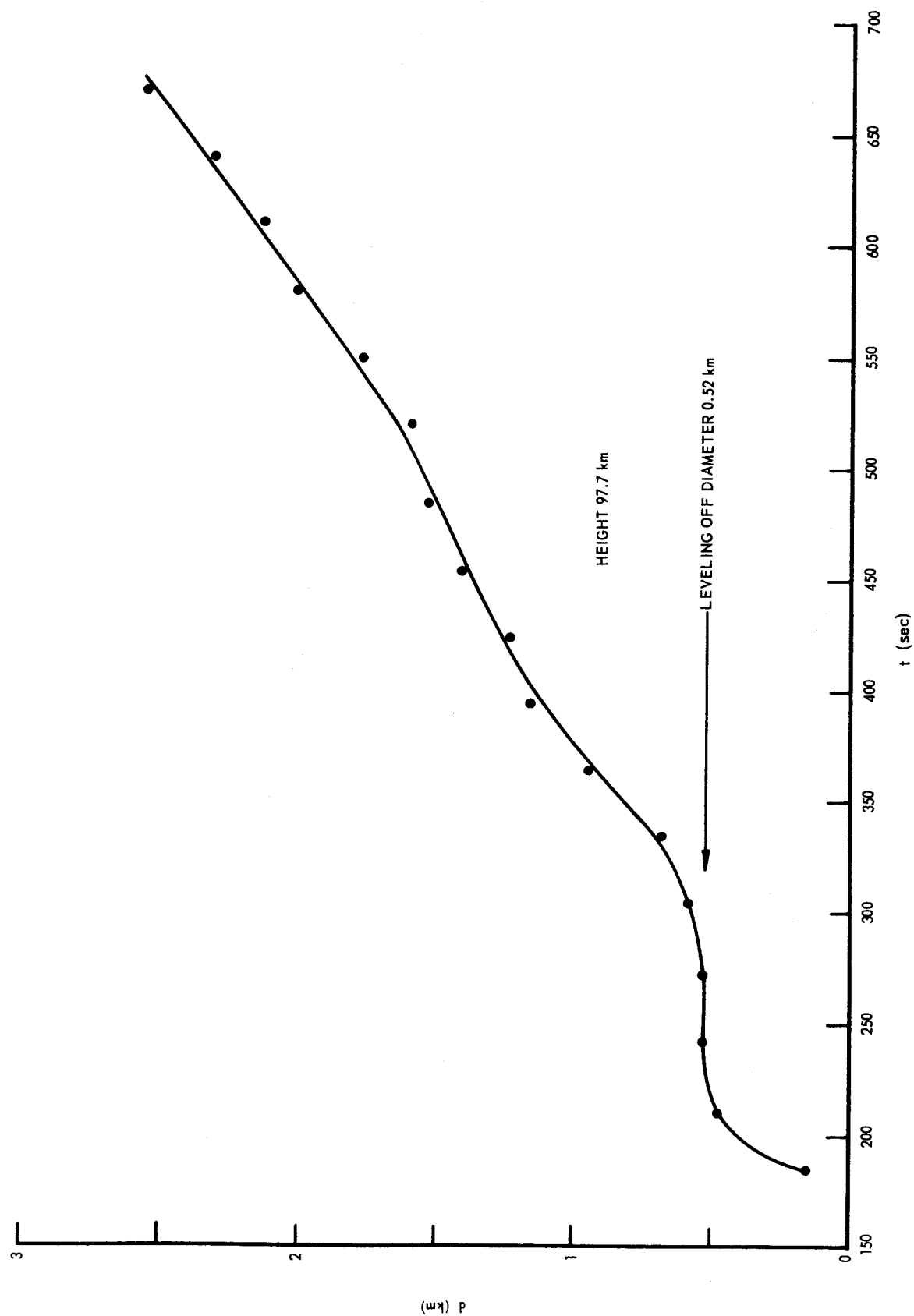


Figure 9. Globule Growth Curve - Diameter Versus Time.

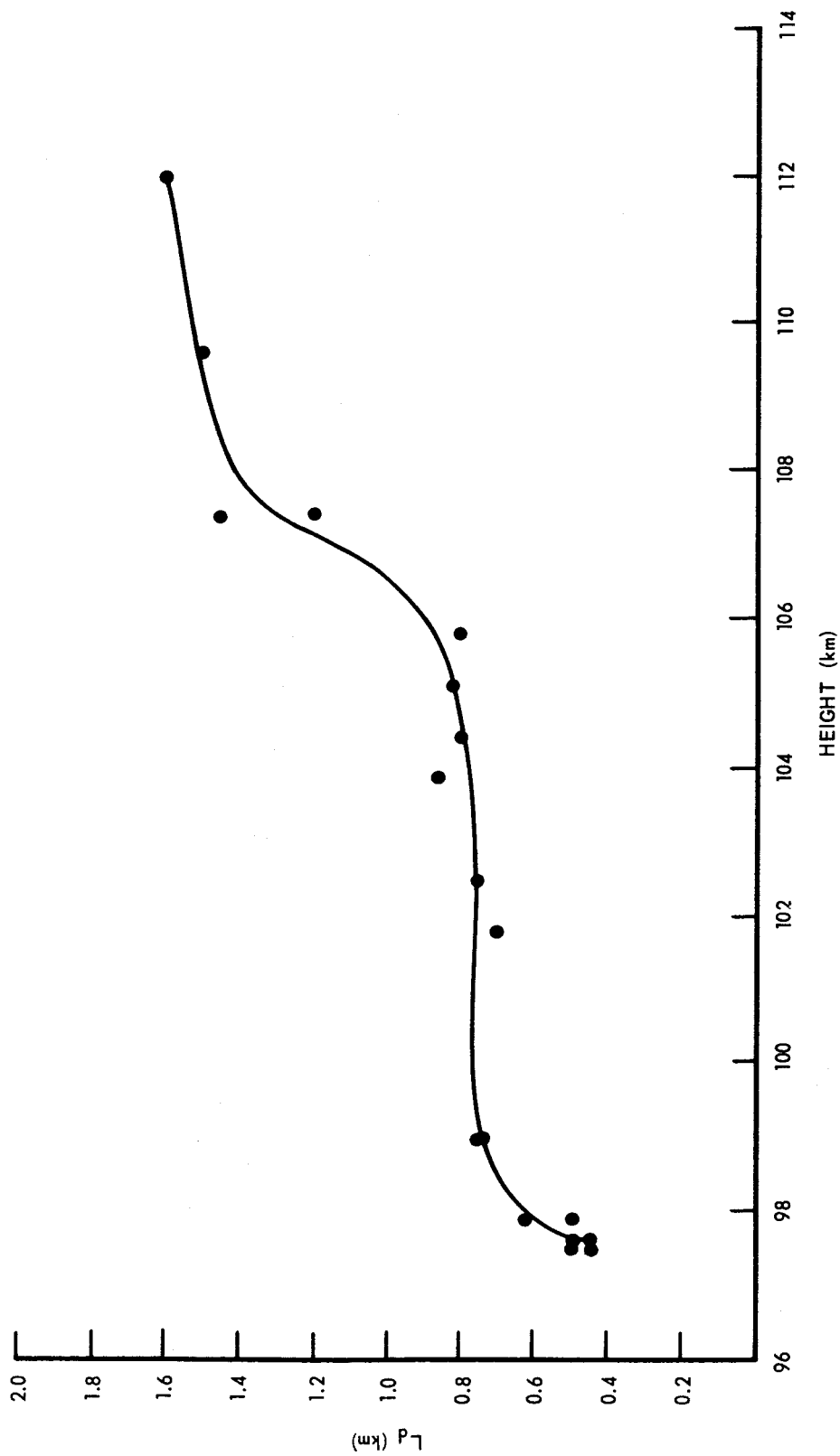


Figure 10. Leveling-off Diameter Versus Altitude.

$H_t$  to be 106.5 and 107.0 km, and the down trails indicated  $H_t$  values of 104.3 and 105.2 km. In both cases  $H_t$  on the down trail showed a shift of 2 km downward with respect to the up trail. This may not be significant because solid particles which followed the trajectory and reentered the atmosphere made the down trails at  $H_t$  more difficult to observe and so the down trail values are much less accurate. It is interesting to note, however, that there appears to be about a 2 km downward shift of the wind pattern of the down trail with respect to the up trail, and this apparent shift in  $H_t$  may be associated with the similar shift in the wind profile.

#### Time Scales of the Motion

In addition to size scales of the motion one can speak of time scales of the motion. The time scale of a particular size scale of eddy would be the time over which that size eddy maintains its identity, or the time over which the turbulent velocity fluctuations maintain some degree of correlation. The size scale,  $L$ , the time scale,  $t_1$ , and the characteristic velocity fluctuation,  $v$ , of the eddy should be related by

$$L = v t_1 \quad (21)$$

according to Batchelor (1953).

The time correlation coefficient of, say, the  $u$  component of turbulent velocity would be

$$g(\delta t) = \frac{\sum [u(t) u(t + \delta t)]}{[\sum u^2(t) \sum u^2(t + \delta t)]^{\frac{1}{2}}} \quad (22)$$

where the summations extend over all observations separated by a time interval  $\delta t$ .

Greenhow and Neufeld (1959b, 1960) report results of an analysis using (22) to calculate time correlation of the turbulent winds. In this analysis the winds were averaged over twenty minute intervals, a harmonic analysis was made of these winds to determine prevailing, diurnal and semi-diurnal components, and the turbulent winds were defined as the residual from the 20 minute average winds after subtracting off the harmonic functions. The first zero of the time correlation coefficient is at  $\delta t \approx 100$  min according to the Greenhow and Neufeld data. This value, they point out, verifies (21) if one uses  $L = 150$  km and  $v = 25$  m/sec which are appropriate figures for the large eddies according to their data.

Again, however, the definition of turbulent winds employed by Greenhow and Neufeld may mean that their value for  $t_1$  applies not to the turbulent winds but more closely to the mean winds. The data of Greenhow and Neufeld (1956, 1960) as well as other meteor investigations indicate that the semi-diurnal component is the one of largest magnitude. This is confirmed by observations by Rosenberg and Edwards (1964) of winds throughout the night determined by a series of chemical release trails. The semi-diurnal component, having a period of 12 hours, would have a zero on the time correlation curve for  $\delta t = 3$  hrs = 180 min. Actual calculation of the time correlation coefficient from the chemical release wind data shows that the first zero on the correlation curve of the mean winds is at about 200 min.

If we assume (21) is valid and use  $L = 6$  km and  $v = 15$  m/sec as indicated by the chemical release data then  $t_1 \approx 400$  sec. Investigation is underway to determine if motions of this time scale are detectable.

The time scale,  $\tau$ , of the smallest eddies can be determined by an equation



complementary to (8)

$$\tau = (\eta/\epsilon)^{\frac{1}{2}} \quad (23)$$

where, as in (8),  $\eta$  is the kinematic viscosity and  $\epsilon$  is either  $\epsilon_t$ , the energy dissipated as heat, or  $\epsilon_s$  the energy supplied by the shears. Tables 4 and 5 show several values of  $\tau$  deduced from both  $\epsilon_s$  and  $\epsilon_t$  for the height range 92-108 km. Both tables show  $\tau$  to be on the order of 10 sec over this height interval. The values given for the velocity fluctuations,  $v_e$ , of the small eddies are calculated from (21) using the appropriate size scales from Tables 1 and 2.

TABLE 4  
VALUES OF  $\tau$  FROM  $\epsilon_s$

Height (km)	$\eta$ (m <sup>2</sup> /sec)	$\epsilon_s$ (m <sup>2</sup> /sec <sup>3</sup> )	$\tau$ (sec)	$v_e$ (m/sec)
92	5.7	0.30	4	1
100	28	0.37	9	2
108	120	0.46	16	3

TABLE 5  
VALUES OF  $\tau$  FROM  $\epsilon_t$

Height (km)	$\eta$ (m <sup>2</sup> /sec)	$\epsilon_t$ (m <sup>2</sup> /sec <sup>3</sup> )	$\tau$ (sec)	$v$ (m/sec)
92	5.7	0.012	22	0.5
100	28	0.14	14	1
108	120	1.1	10	3

SUMMARY

Table 6 and 7 give a summary of the various size scales of the motion and tabulate their magnitudes or range of values in the indicated height interval. If no height interval is indicated the applicable interval is probably 90-110 km.

TABLE 6  
SIZE SCALES OF THE MEAN MOTION

Scale Description	Symbol Used	Magnitude (km)	Height Range (km)
Horizontal Scale		150 - 1000	≈ 90 - 140
Vertical			
Autocorrelation Scale	$L_v$	4.3 - 8.6	81 - 130
"	$L_{v1}$	4.1 - 6.5	"
"	$L_{v2}$	2.4 - 4.5	"
Motion Spectrum Scale	$L_s$	5.5 - 12.0	83 - 127

TABLE 7  
SIZE SCALES OF THE TURBULENT MOTION

<u>Scale Description</u>	<u>Symbol Used</u>	<u>Magnitude</u> (km)	<u>Height Range</u> (km)
Vertical and Horizontal Scale of Largest Eddies from Correlation Coefficient	$L_o$	6	
Integral Scale of Correlation Curve	$L_i$	1	
Mixing Length Scale	$L_m$	0.7 - 3.3	92 - 113
Dissipation Length (a) from correlation coefficient	$L_p$	0.6	
(b) from turbulent winds	$L_t$	0.65	93 - 109
Globule Size Spectrum Peak		0.7 - 1.2	
Globule Leveling Off Diameter	$L_d$	0.8 - 1.5	
Isotropic Subrange (a) from (18)	$l_i$	0.022 - 0.97	90 - 115
(b) from globule shapes		$\approx 1$	90 - 110
Scale of Smallest Eddies			
(a) from energy dissipation rate	$l_e$	0.011 - 0.035	92 - 108
(b) from energy supplied by shears	$l_e$	0.005 - 0.044	92 - 108
(c) from correlation coefficient	$l_c$	0.018	

The motion has been separated here into mean winds and turbulent fluctuations. However if no restricting conditions were imposed on the flow field, motions considered here as mean winds could (after subtracting off any tidal or other non-random components) be considered as the turbulent component for higher order size and time scale eddies.

If a fluid element is displaced a small amount from its equilibrium position, it experiences a restoring force which produces a harmonic motion with a natural frequency  $\omega_g$ , the Brunt-Väisälä frequency, given by (19). Layzer (1961) states that if the lifetime  $t_1$  of a turbulent eddy is greater than  $2\pi/\omega_g$ , then it is possible to follow a typical fluid element throughout a complete gravitational oscillation. But if a fluid element retains its identity for such a length of time the motion is not true turbulence. Again using the value  $\omega_g = 2.4 \times 10^{-2} \text{ sec}^{-1}$  we see that motions with time scales great than about 260 seconds would not be true turbulence.

This value of  $\omega_g$  may be in error since it is based on standard atmosphere conditions and an extrapolation of  $C_p$  from the values for air at low pressure laboratory conditions. Table 8 shows the values of  $\partial T / \partial z$  and  $g/C_p$  which are the two least accurately known terms in  $\omega_g$ . It is seen that in the range 90-115 km the  $g/C_p$  term contributes more heavily to  $\omega_g$  than the  $\partial T / \partial z$  term. Thus a large uncertainty in  $g/C_p$  would represent a correspondingly large uncertainty in  $\omega_g$ . Consequently it may be that values of  $t_1 \approx 400 \text{ sec}$ , previously deduced from the chemical release winds, would represent true turbulent motion. But it would be difficult to reconcile a turbulent motion with a time scale of 100 minutes or more with the above argument.

TABLE 8  
 $\frac{\partial I}{\partial z}$  AND  $g/C_p$  VERSUS HEIGHT

$\frac{z}{(km)}$	$\frac{\partial I}{\partial z}$ $(o_K/km)$	$\frac{g}{C_p}$ $(o_K/km)$
90	0.00	9.54
95	2.94	9.53
100	3.85	9.51
105	4.70	9.49
110	7.00	9.47
115	9.25	9.43

It seems quite likely that the features of the mean winds can be explained by a combination of tidal waves and other ordered motion such as the gravity waves proposed by Hines (1959, 1960). If this is the case then true turbulence will be confined to the size and time scales discussed here as being associated with the turbulent motion. Further work must be done, however, to clarify the exact nature of the motions here described as the mean winds, and to resolve these motions into tidal wave, gravity wave, and other ordered motions which may contribute to the total mean winds.

#### ENERGY BALANCE OF THE MOTION

If the flow is statistically steady the energy balance equation is

$$\epsilon_s = \epsilon_g + \epsilon_t \quad (24)$$

where  $\epsilon_s$  is the rate per unit mass of atmosphere at which the turbulence extracts energy from the wind shears of the mean flow,  $\epsilon_g$  is the rate per unit mass of atmosphere at which the turbulence does work against gravity, and  $\epsilon_t$  is the rate per unit mass of atmosphere at which turbulent energy is dissipated as heat by viscous effects. The rate of supply  $\epsilon_s$  is given by

$$\epsilon_s = \sum_i \sum_j u_i u_j \frac{\partial U_i}{\partial x_j} \quad (25)$$

where the  $U$ 's are components of the mean velocity, the  $u$ 's are components of the turbulent velocity and the  $x$ 's are coordinates,  $x_3$  being the vertical coordinate, and  $x_1$  and  $x_2$  appropriate horizontal coordinates. An order of magnitude relations for  $\epsilon_s$  is

$$\epsilon_s \approx \frac{v^3}{L} \quad (26)$$

where  $v$  and  $L$  are the characteristic turbulent velocity and scale of the energy containing eddies.

The mixing length theory provides an approximate relation for  $\epsilon_g$

$$\epsilon_g = \overline{u_3 L_m} \omega_g^2 \approx \frac{\overline{u_1 u_3} \omega_g^2}{\left( \frac{\partial U_1}{\partial x_3} \right)} \quad (27)$$

where  $L_m$  is the mixing length given by (7) and  $\omega_g$  is the Brunt-Vaisala " " " frequency given by (19).

According to Lamb (1945) the general expression for  $\epsilon_t$  is

$$\epsilon_t = \eta \left[ 2 \sum_i \left( \frac{\partial u_i}{\partial x_i} \right)^2 + \sum_{cyc} \left( \frac{\partial u_1}{\partial u_3} + \frac{\partial u_3}{\partial u_1} \right)^2 \right] - \frac{2\eta}{3} \left( \sum_i \frac{\partial u_i}{\partial x_i} \right)^2 \quad (28)$$

where  $\eta$  is the kinematic viscosity and  $\sum_{\text{cyc}}$  indicates summation over a full

cyclic permutation of indices. If the atmosphere is assumed incompressible then  $\sum_i \frac{\partial u_i}{\partial x_i} = 0$ , from the continuity equation, so the last term in (28)

would disappear. If, in addition, the turbulence is assumed to be isotropic then it can be shown (Taylor (1935) ) that

$$\epsilon_t = 6 \eta \left[ \overline{\left( \frac{\partial u_1}{\partial x_1} \right)^2} + \overline{\left( \frac{\partial u_1}{\partial x_2} \right)^2} + \overline{\frac{\partial u_2}{\partial x_1} \frac{\partial u_1}{\partial x_2}} \right] \quad (29)$$

which can be reduced to

$$\epsilon_t = \frac{15}{2} \eta \overline{\left( \frac{\partial u_1}{\partial x_2} \right)^2} \quad (30)$$

since the terms in (29) are not all independent for an isotropic field and incompressible flow.

The turbulent wind components of wind data obtained from chemical release clouds may be used in (25) and in (27) through (30) to evaluate  $\epsilon_s$  and  $\epsilon_g$  and give three separate evaluations of  $\epsilon_t$ . For this procedure averages such as  $\overline{u_i u_j}$  are obtained by averaging over all wind determinations in a finite height interval, usually about 2 km. The derivatives are approximated by ratios of finite differences  $\Delta u_i / \Delta x_j$ . The results of these evaluations of the energy terms, shown in Figure 12, will be discussed later in this report.

The manner in which a cloud of material diffuses after injection into the turbulence offers another method for evaluating  $\epsilon_t$ . Cote (1962) summarizes the theoretical results of several authors, Lin (1960), Tchen (1961), Bolgiano (1959) and Roberts (1960) for the dispersion law that should be followed by the diffusing material. The various dispersion relations are

$$\langle r^2 \rangle \sim (t - t_0)^2 \quad (31)$$

$$\langle r^2 \rangle \sim \epsilon_t (t - t_0)^3 \quad (32)$$

$$\langle r^2 \rangle \sim \epsilon_t^2 (t - t_0)^4 \quad (33)$$

$$\langle r^2 \rangle \sim Z (t - t_0)^5 \quad (34)$$

$$\langle r^2 \rangle \sim \epsilon_t^4 (t - t_0)^6 \quad (35)$$

where  $\langle r^2 \rangle$  is the mean square separation between particles of the injected material,  $t_0$  is some appropriate reference time, presumably the time of injection, and  $Z$  in (34) is a function of the atmospheric potential density fluctuation and the vertical turbulent velocity fluctuations. The relations (31), (32), (33), and (35) result from the use of different forms of the theoretical energy spectrum function, which gives a description of the distribution of the energy within the energy containing eddies. Formula (34) is based on Bolgiano's theory, mentioned in a previous section.

The relation (32) was first deduced by Batchelor (1950) from Kolmogoroff's similarity hypothesis. It is this form of dispersion which presumably holds if Kolmogoroff's principle is valid. The complete relation for describing the diffusion of a cloud injected into the turbulent field would be

$$d^2 = \frac{16}{3} \epsilon_t (t - t_0)^3 \quad (36)$$

where  $d$  is the diameter of the cloud, or trail of material.

Figure 11 shows a plot on log-log scale of the diameter squared of a globule versus  $t - t_0$ . This is the growth curve for the same globule shown in Figure 9. It is seen that the points at early times when the globule is going through the leveling off phase do not follow a power law, but above the leveling off size the growth follows the relation (36) closer than any other



of the diffusion formulas, the actual exponent being 2.62 in this case.

Each of the formulas (31), (32), (33) and (35) is of the form

$$\langle r^2 \rangle \sim \epsilon_t^{\alpha-2} (t - t_0)^\alpha. \quad (37)$$

If the 16/3 factor of (36) is assumed, a least squares fit of globule growth data to the formula

$$d^2 = 16/3 \epsilon_t^{\alpha-2} (t - t_0)^\alpha \quad (38)$$

can be made by assuming some reasonable value of  $t_0$ . This procedure allows solution for both  $\alpha$  and  $\epsilon_t$ . The average value thus obtained for  $\alpha$  was  $3.0 \pm 0.4$  rms. The resultant  $\epsilon_t$  data are shown in Figure 12.

Data were available primarily in the region from 92-108 km for using in (25), (27) through (30), and (37). A small amount of data were also available in the range 108-112 km. Functions of the arbitrary form  $\epsilon = \exp(a + bz)$  were fit through the data obtained by each of these procedures. The resultant curves, straight lines on a semi-log plot, are shown in Figure 12. The curves from each of the three turbulent wind methods for evaluating  $\epsilon_t$  disagree among themselves at some altitudes by about a factor of five, and the results from (29) and (30), which should yield identical values of  $\epsilon_t$  for isotropic incompressible flow, disagree at some altitudes by about a factor of 2. The curve for  $\epsilon_t$  obtained from globule growth rates is in rather poor agreement with the other  $\epsilon_t$  data, especially at low altitudes. There was considerable scatter, however, in the data points for  $\epsilon_t$  from globule growth, some of the individual data points actually falling in the region of the other three  $\epsilon_t$  curves. All of the four  $\epsilon_t$  curves show  $\epsilon_t$  increasing rapidly with

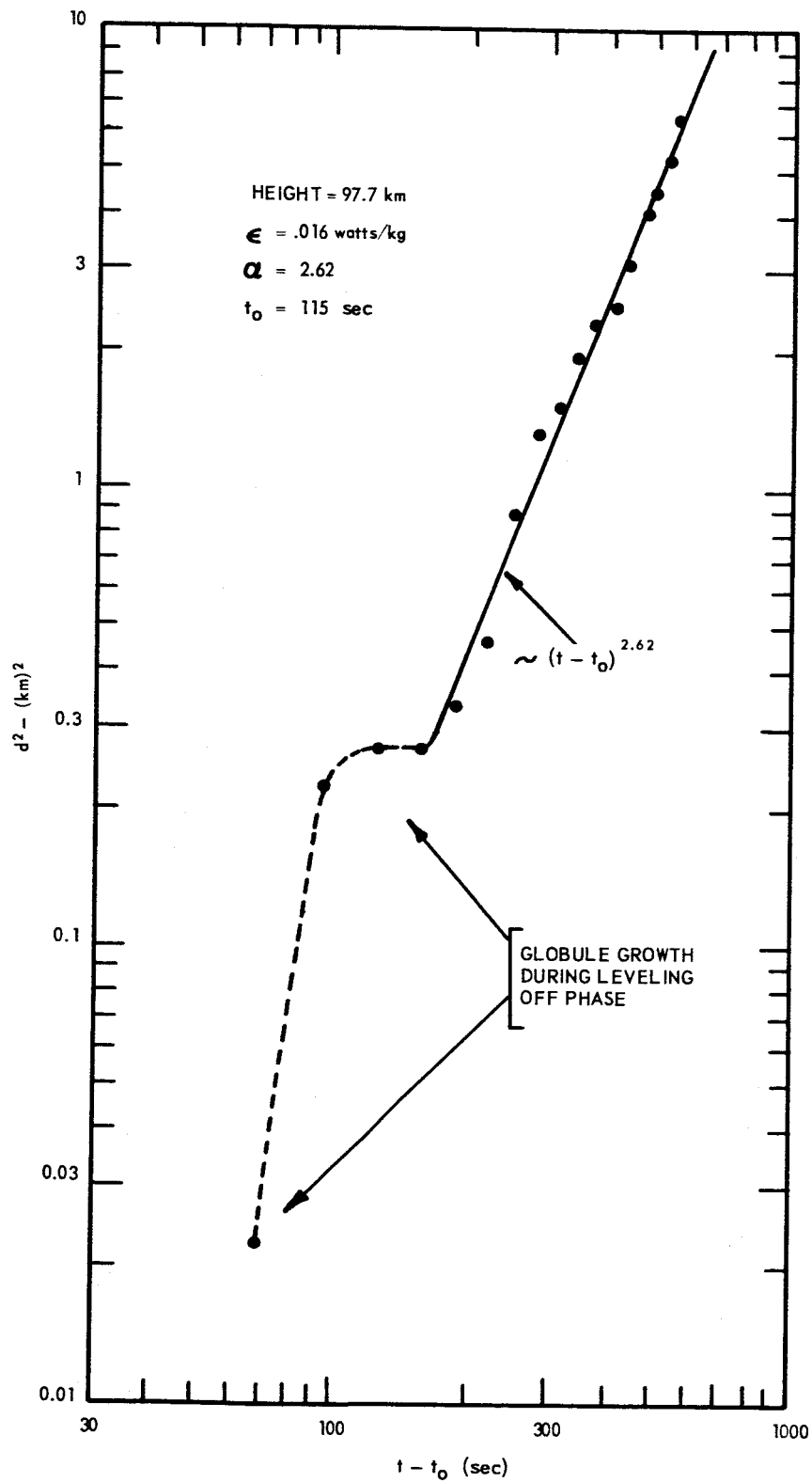


Figure 11. Globule Growth on Log-Log Scale - Diameter Squared Versus Time.

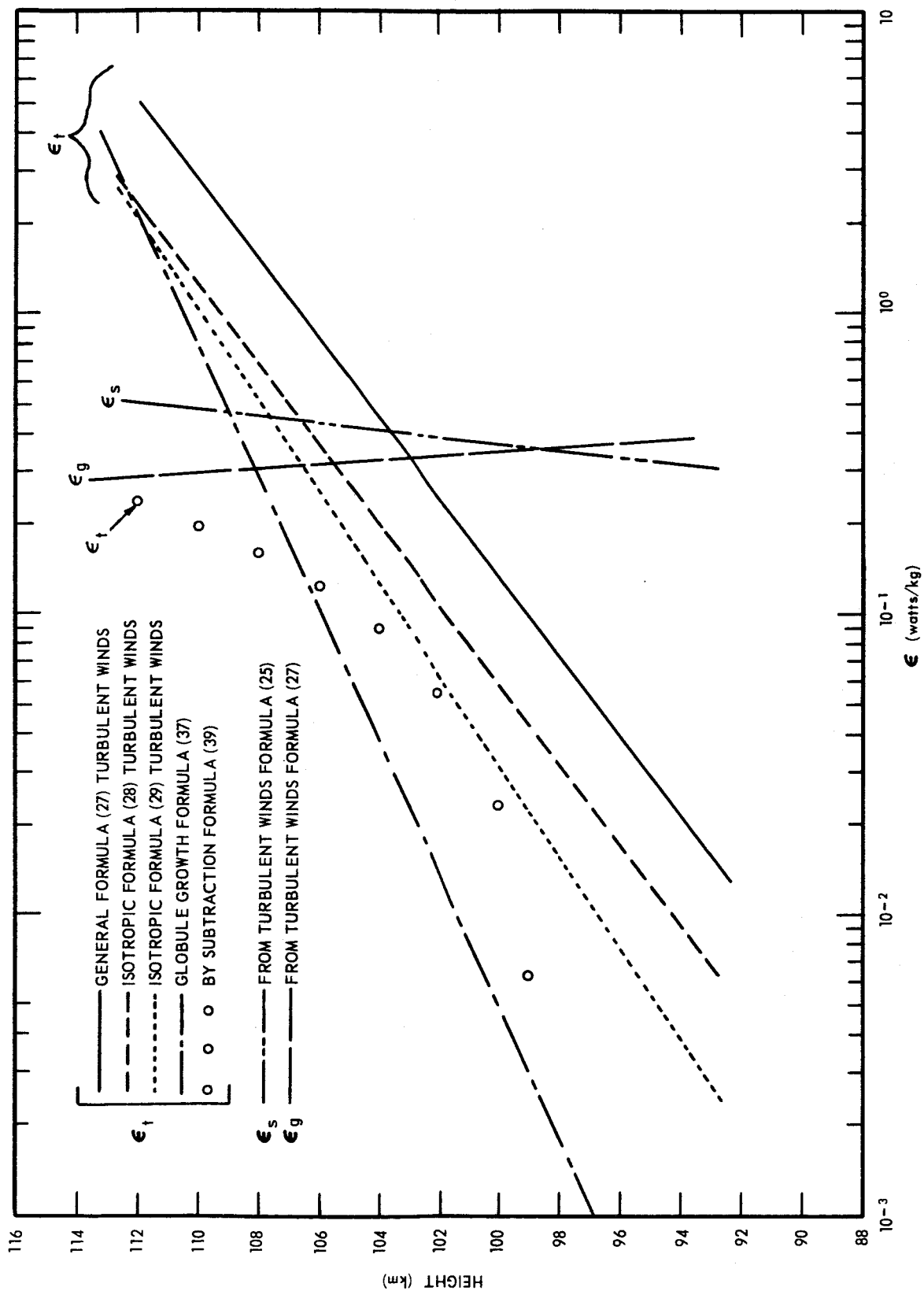


Figure 12. Variations of Energy Balance Terms with Altitude.

altitude, changing by two orders of magnitude or more in 15 km.

The curves for  $\epsilon_s$  and  $\epsilon_g$  show comparatively little variation with altitude. The actual curve for  $\epsilon_g$  is greater in magnitude than  $\epsilon_s$  from 98½ km down, which is physically unreasonable, but it should be realized that each of the curves  $\epsilon_s$  and  $\epsilon_g$  should have an uncertainty of about a factor of two at each altitude. This  $\epsilon_g > \epsilon_s$  anomaly can be rectified well within these limits of accuracy. It should be noted that an additional estimate of  $\epsilon_t$  obtained by subtraction of the  $\epsilon_g$  curve from the  $\epsilon_s$  curve by

$$\epsilon_t = \epsilon_s - \epsilon_g \quad (39)$$

agrees reasonably well with the other values for  $\epsilon_t$  in the height range from 100 to 108 km.

The point at which the  $\epsilon_t$  curve intersects the  $\epsilon_s$  curve should represent the absolute upper limit for the existence of turbulence, since at this intersection point the rate of energy supply would be equal to the rate of energy being dissipated by viscous effects alone. The heights of these intersection points for the various  $\epsilon_t$  curves range from 104 to 109 km, with 107 km representing an approximate mean. This 107 km altitude agrees with the observed average value of 106 km for the turbopause altitude.

If the values  $v = 15$  m/sec and  $L = 6$  km are used in (26) as the appropriate values of rms turbulent velocity and scale, as determined from the chemical release wind data, one obtains the value  $\epsilon_s \approx 0.6$  watts/kg. Similarly if one uses in (27) mean values of  $\overline{u_1 u_3} = .11 \text{ m}^2/\text{sec}^2$ ,  $\omega_g^2 = 6 \times 10^{-4} \text{ sec}^{-2}$  and  $\partial U_1 / \partial x_3 = 20 \text{ m/sec km}$ , which are approximate average values for these quantities throughout the height range 90 - 110 km, one obtains  $\epsilon_g \approx 0.3$  watts/kg. Both

of these estimated values agree fairly well with the curves for  $\epsilon_s$  and  $\epsilon_g$  in Figure 12.

Figure 13 shows a summary by Lettau (1961) of values obtained for  $\epsilon_t$  from diffusion and wind profile observations in the altitude range from 1 cm to 40 km. The figure also illustrates the  $\epsilon_t$  variation versus altitude as determined from the chemical release diffusion and wind data in the approximate height range 90 to 110 km. It appears from Figure 13 that  $\epsilon_t$  continues to decrease with decreasing altitude below 90 km, diminishing by an additional 3 or more orders of magnitude from 90 to 30 km.

#### CRITERIA FOR THE ONSET OF TURBULENCE

##### Reynolds Criterion

Working on flow experiments in long, straight pipes, Reynolds showed in 1883 that the motion became turbulent when the Reynolds number exceeded a critical value ( $\approx 2000$ ). The Reynolds number is defined as

$$R_e = \frac{ud}{\eta} \quad (40)$$

where  $u$  is the flow velocity,  $d$  is the pipe diameter and  $\eta$  is the kinematic viscosity.

In the free atmosphere it is stability that primarily determines whether or not turbulence is present. If temperature decreases with altitude so that the region is gravitationally unstable the velocity gradient will almost never be so small that turbulence will be inhibited by a low Reynolds number. When the region is gravitationally stable the flow will be laminar in weak velocity gradients, but if the velocity gradient is sufficiently large the region will be turbulent in spite of the gravitational stability.

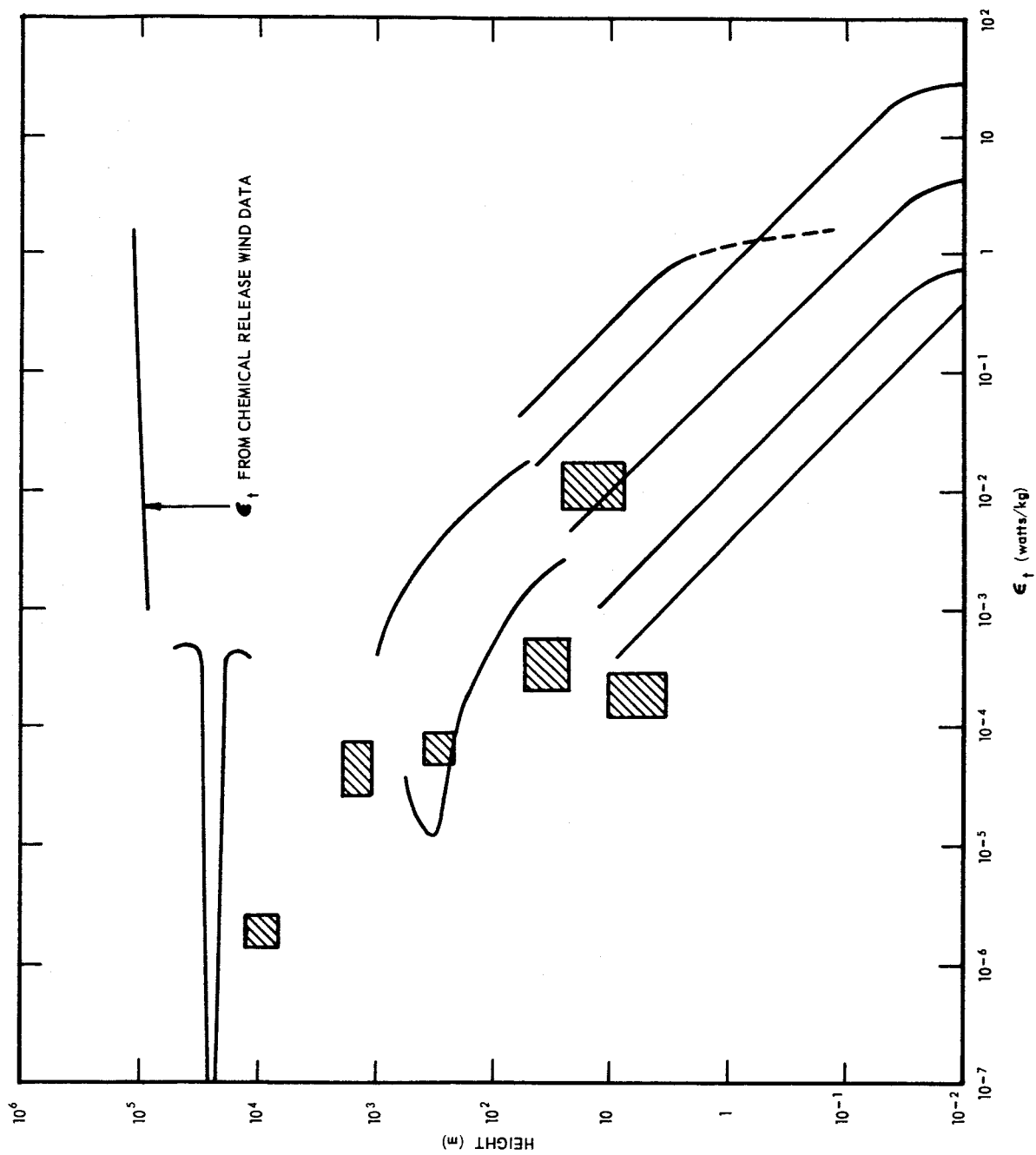


Figure 13. Viscous Energy Dissipation Rate from Altitudes of 1 cm to 110 km.

Consequently the Reynolds number has little bearing on the existence of turbulence in the height region above 85 km and we must examine other criteria for the onset of turbulence.

#### Richardson's Criterion

Richardson's theory (1920) is based on the assumption that if  $\epsilon_t > 0$  turbulence exists. From (24) it is seen that this condition is equivalent to  $\epsilon_s - \epsilon_g > 0$  or  $\epsilon_g/\epsilon_s < 1$ . Using the approximation

$$\epsilon_s = \left| \overline{uw} \right| \frac{\partial U}{\partial z} \quad (41)$$

Richardson's forms for  $\epsilon_s$  and  $\epsilon_g$  are

$$\epsilon_s = K_E \omega_s^2 \quad (42)$$

$$\epsilon_g = K_C \omega_g^2 \quad (43)$$

where  $\omega_s = \partial U / \partial z$ . From the equations (27) and (41) it is seen that  $K_C = \overline{wL_m}$ , and  $K_E = \overline{uw} / (\partial U / \partial z)$  or, using the mixing length theory,  $K_E$  is defined by

$$K_E = L_m^2 \left( \frac{\partial U}{\partial z} \right)^2. \quad (44)$$

Richardson assumed  $K_E = K_C$  so that the condition  $\epsilon_g/\epsilon_s < 1$  is equivalent to the Richardson number,  $R_i$ , being less than 1, where the Richardson number is defined by

$$R_i = \frac{\omega_g^2}{\omega_s^2} \quad (45)$$

Therefore the Richardson criterion may be outlined as

$$\begin{array}{ll}
R_i < 1 & \text{turbulent} \\
R_i > 1 & \text{laminar.}
\end{array} \tag{46}$$

### Townsend's Criterion

Townsend (1957) developed a more elegant criterion for turbulence based on an analogy between turbulent motion and Brownian motion. For this theory the quantity  $\omega_t$  defined by

$$\epsilon_t = (\overline{u^2} + \overline{v^2} + \overline{w^2}) \omega_t \tag{47}$$

is important. Using the Brownian motion analogy, Townsend arrives at the result

$$\overline{wL}_m = \frac{\overline{w^2}}{2\omega_t} . \tag{48}$$

Using this in (43),  $\epsilon_g$  may be written

$$\epsilon_g = \frac{1}{2} k_g \overline{w^2} \frac{\omega_g^2}{\omega_t}$$

where  $k_g = 1$  if the Brownian motion analogy holds exactly, so  $k_g$  should be a constant close to unity.

Equations (47) and (42) are rewritten as

$$\epsilon_t = \frac{3}{2} k_t \overline{w^2} \omega_t \tag{49}$$

and

$$\epsilon_s = \frac{2}{5} k_s \overline{w^2} \omega_s \tag{50}$$

where the coefficients  $k_t$  and  $k_s$  are of order unity.



Defining the Richardson flux number,  $R_f$ , as

$$R_f = \frac{\epsilon_g}{\epsilon_s} \quad (51)$$

Townsend derives the result

$$(1 - R_f)R_f = \frac{75}{16} \frac{k_g k_t}{k_s^2} R_i \quad (52)$$

The left hand side of (52) is a minimum at  $R_f = \frac{1}{2}$  and at this point  $R_i$  is the critical value  $R_{ic}$  given by

$$R_{ic} = \frac{4}{75} \frac{k_s^2}{k_g k_t} \approx 0.05. \quad (53)$$

The flow will be turbulent for all  $R_i < R_{ic}$ .

#### Layzer's Criterion

Layzer (1961) extended the ideas of Townsend by imposing the additional restriction  $\omega_t > \omega_g$ . This is the same condition  $t_1 < 2\pi/\omega_g$  discussed in the section on time scales of the motion. For this to be true it is necessary that the condition

$$R_f < \frac{k_g}{k_g + 3k_g} \quad (54)$$

be true. Combining (52) and (54), Layzer derives the condition

$$R_i < R_{ic} = \frac{4}{5} \left( \frac{k_s}{k_g + 3k_g} \right)^2 \approx 0.05 \quad (55)$$

where, again, the flow will be turbulent for all  $R_i < R_{ic}$ .

#### Observations on Chemical Release Wind Data

Townsend's and Layzer's interia are designed to eliminate quantities such as  $\overline{uw}$  and  $\overline{u^2}$  which are considered unknowns. The mathematical steps of these

theories can be retraced making only the assumption

$$wL_m = \frac{k_j \overline{w^2}}{\omega_t} \quad (56)$$

where  $k_j$  is of order unity. Starting with equations (27), (41), and (47), if all the quantities involving turbulent velocity fluctuations are retained then the modified Townsend and Layzer criteria are

$$R_i < \frac{8(\overline{uw})^2}{(\overline{u^2} + \overline{v^2} + \overline{w^2})k_j \overline{w^2}} \quad (\text{Townsend}) \quad (57)$$

$$R_i < \frac{4(\overline{uw})^2}{[\overline{u^2} + \overline{v^2} + \overline{w^2}(1 + 2k_j)]^2} \quad (\text{Layzer}) \quad (58)$$

Each of these critical values is on the order of 0.01 for the wind data obtained from the chemical releases.

The average Richardson number in the height range 90-110 km is on the order of unity, however, so that there is little chance of satisfying Townsend's or Layzer's criteria in this altitude region. The percentage occurrence of Richardson number less than one have been calculated for the chemical release wind data and the results are shown in Figure 14. It is seen that the maximum occurrence is around 105 km,  $R_i$  being less than 1 about 35 percent of the time there. At 125 km the occurrence of  $R_i < 1$  has fallen virtually to zero and at 90 km  $R_i$  is less than 1 only about 10 percent of the time.

#### CONCLUSIONS

From the data presented here it seems that the turbulence observed up to altitudes near 105 km is ambient turbulence produced by wind shears, and is

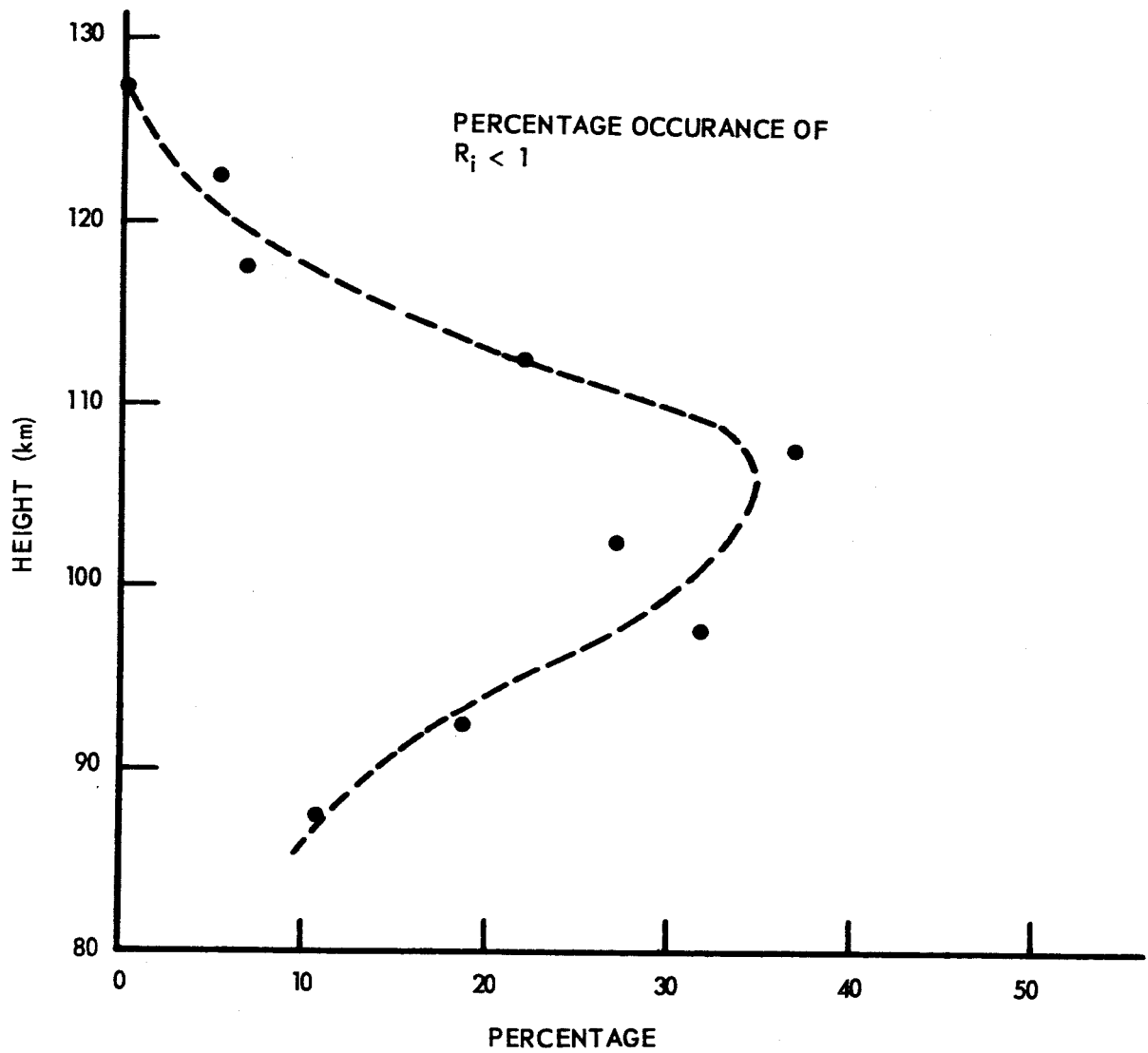


Figure 14. Percentage Occurance of  $R_i < 1$  Versus Altitude.

isotropic only for scales  $\approx 1$  km or less. The smallest eddies are on the order of 20 m in size with characteristic velocities and times of about 2 m/sec and 10 sec. The largest eddies are about 6 km in size with characteristic velocities and times of about 15 m/sec and 400 sec. The winds which over short time intervals are considered to be the mean winds may have turbulent components of larger horizontal scale than 6 km, and longer time scale than 400 sec, but probably tidal waves and gravitational waves account for most of the fluctuations of this scale.

There are four parameters of the turbulence that depend on the factor  $\omega_g$ . They are: 1) the scale of isotropy,  $l_i$ , in (18); 2) the time scale,  $t_g$ , of gravitational oscillations given by  $t_g = 2\pi/\omega_g$ ; 3) the gravitational term in the energy balance,  $\epsilon_g$ , in (27); 4) the Richardson number,  $R_i$ , in (45). The conclusions of the previous paragraph would be strengthened if  $l_i$  and  $t_g$  were larger and if  $R_i$  and  $\epsilon_g$  were smaller than the calculated values. All of these conditions would require  $\omega_g$  to be smaller than the calculated value. It may be that equation (19) for  $\omega_g$ , which is based on standard thermodynamic laws, is not applicable to the near plasma conditions of the 100 km height region, or if (19) is valid, the presumed values of  $C_p$  may not be applicable at this altitude.

The upper height limit of turbulence of size scale less than 6 km usually occurs within  $\pm 5$  km of the 105 km level. From the data presented here it appears that this cutoff altitude, or turbopause, is caused by the rate of energy supplied by wind shears becoming too small to maintain the turbulence in the presence of dissipation rates which are increasing rapidly with altitude.

The Batchelor form of turbulent diffusion (32) has been shown as most corresponding to observed growth rates of individual globules. The actual exponent observed for the diffusion power law was  $3.0 \pm 0.4$  rms. Cote (1962) has measured diffusion rates of chemical release trails. He reported that, without further study, it could not be shown conclusively whether or not the diffusion power law observed for the trails was different from the  $d^2 \sim t^2$  relation expected for diffusion of a turbulent wake or turbulent jet. Wake or jet type diffusion would presumably be produced by rocket generated turbulence.

No turbulent diffusion measurements on the expansion of complete trails have been made yet by this group but work is underway on such measurements. If an exponent of 3 were observed for diffusion of trails as well as of individual globules, this would definitely rule out the possibility that the observed turbulence is in any way produced by the rocket or the ejection mechanism.

Further investigations of the spatial and time correlations of the turbulent wind components are planned. In particular, more accurate approximations to the one dimensional correlation coefficients  $g_{ii}$  will be evaluated, and a search for motion fluctuations of the expected time scale of 400 sec will be carried out.

Preliminary results indicate that Tchen's theory (1954) is applicable to the motion and energy spectrum of the mean winds for vertical separations, but that a Kolmogoroff motion spectrum may be followed if total spatial separation is considered in the evaluation of the spectrum function.

In addition, it is hoped that future work can establish what portions of the mean wind features are attributable to tidal wave, gravitational wave, and possibly large scale turbulent components.

# REFERENCES

1. Albritton, D. L., L. C. Young, H. D. Edwards, and J. L. Brown, Photogrammetric Engineering, 28, 608 (1962)
2. Batchelor, G. K., Proc. Cambridge Phil. Soc., 43, 533 (1947)
3. Batchelor, G. K., Quart. Jour. Roy. Met. Soc., 76, 133 (1950)
4. Batchelor, G. K., Homogeneous Turbulence (1953)
5. Blamont, J. E. and C. de Jager, Annales de Geophys., 17, 134 (1961)
6. Blamont, J. E. and C. de Jager, Jour. Geophys. Res., 67, 3113 (1962)
7. Bolgiano, Jr., R., Jour. Geophys. Res., 64, 2226-2229 (1959)
8. Bolgiano, Jr., R., Jour. Res. Nat. Bur. Stand., 64D, 231 (1960)
9. Cote, O., "On the Question of Turbulence in the Upper Atmosphere," (NASA Rept.) GCA Tech. Rept. No. 62-12-N (1962)
10. Dougherty, J. P., Jour. Atm. Terr. Phys., 21, 210-213 (1961)
11. Edwards, H. D., M. M. Cooksey, C. G. Justus, R. N. Fuller, D. L. Albritton, and N. W. Rosenberg, Jour. Geophys. Res., 68, 3021 (1963)
12. Greenhow, J. S. and E. L. Neufeld, Phil. Mag., 1, 1157 (1956)
13. Greenhow, J. S. and E. L. Neufeld, Proc. Phys. Soc. (London), 74, 1 (1959a)
14. Greenhow, J. S. and E. L. Neufeld, Jour. Geophys. Res., 64, 2139 (1959b)
15. Greenhow, J. S. and E. L. Neufeld, Proc. Phys. Soc. (London), 75, 228 (1960)
16. Hines, C. O., Jour. Geophys. Res., 64, 2210 (1959)
17. Hines, C. O., Can. Jour. Phys., 38, 1441, (1960)
18. Justus, C. G., H. D. Edwards, and R. N. Fuller, "Analysis Techniques for Determining Mass Motions in the Upper Atmosphere from Chemical Releases," Scientific Report AFCRL-64-187 (1964a)
19. Justus, C. G., H. D. Edwards, and R. N. Fuller, Photogrammetric Engineering, in print (1964b)
20. Kolmogoroff, A. N., Compt. Rend. Acad. Sci. URSS, 30, 301 (1941)
21. Lamb, H., Hydrodynamics (1945)

22. Layzer, D., "The Turbulence Criterion in Stably Stratified Shear Flow and the Origin of Sporadic E," Unpublished Notes, (1961)
23. Lettau, H. H., Jour. Atm. Terr. Phys., 21, 210-213 (1961)
24. Lin, C. C., Proc. Natl. Acad. Sci., 46, 566-570 (1960), 46, 1147-1150 (1960)
25. Nawrocki, P. J. and R. Papa, Atmospheric Processes (1963)
26. Richardson, L. F., Proc. Roy. Soc. (London), A97, 354 (1920)
27. Roberts, P. H., Jour. Fluid Mech., 11, 257-283 (1960)
28. Roper, R. G. and W. G. Elford, Nature, 197, 963 (1963)
29. Rosenberg, N. W. and H. D. Edwards, Jour. Geophys. Res., 69, 2819 (1964)
30. Stewart, R. W., Jour. Geophys. Res., 64, 2112 (1959)
31. Sutton, O. G., Micrometeorology (1953)
32. Taylor, G. I., Proc. Roy. Soc. (London), A151, 430 (1935)
33. Taylor, G. I., Proc. Roy. Soc. (London), 164, 476 (1938)
34. Tchen, C. M., Phys. Rev., 93, 4 (1954)
35. Tchen, C. M., Advances in Geophysics, 6, 165-173 (1961)
36. Townsend, A. A., The Structure of Turbulent Shear Flow (1956)
37. Townsend, A. A., Jour. Fluid Mech., 3, 361 (1957)
38. U. S. Standard Atmosphere (1962)
39. Zimmerman, S. P., Ann. de Geophys., 18, 116 (1962)
40. Zimmerman, S. P., Jour. Geophys. Res., 69, 784 (1964)